EGFR-dependent phosphorylation of leucine-rich repeat kinase LRRK1 is important for proper endosomal trafficking of EGFR

Kouki Ishikawa[a], Atsuki Nara[b], Kunihiro Matsumoto[a], and Hiroshi Hanafusa[a]
[a]Department of Molecular Biology, Graduate School of Science, Nagoya University, Chikusa-ku, Nagoya 464-8602, Japan; [b]Faculty of Bioscience, Nagahama Institute of Bio-Science and Technology, Nagahama, Shiga 526-0829, Japan

ABSTRACT **Ligand-induced activation of the epidermal growth factor receptor (EGFR) initiates trafficking events that relocalize the receptors from the cell surface to intracellular endocytic compartments. We recently reported that leucine-rich repeat kinase 1 (LRRK1) is involved in the trafficking of EGFR from early to late endosomes. In this study, we demonstrate that EGFR regulates the kinase activity of LRRK1 via tyrosine phosphorylation and that this is required for proper endosomal trafficking of EGFR. Phosphorylation of LRRK1 at Tyr-944 results in reduced LRRK1 kinase activity. Mutation of LRRK1 Tyr-944 (Y944F) abolishes EGF-stimulated tyrosine phosphorylation, resulting in hyperactivation of LRRK1 kinase activity and enhanced motility of EGF-containing endosomes toward the perinuclear region. The compartments in which EGFR accumulates are mixed endosomes and are defective in the proper formation of intraluminal vesicles of multivesicular bodies. These results suggest that feedback down-regulation of LRRK1 kinase activity by EGFR plays an important role in the appropriate endosomal trafficking of EGFR.**

Monitoring Editor
Jean E. Gruenberg
University of Geneva

Received: Sep 13, 2011
Revised: Feb 2, 2012
Accepted: Feb 8, 2012

INTRODUCTION

Endocytosis and subsequent delivery of endosomal cargoes to lysosomes are essential for the degradation of many membrane-associated proteins (Katzmann *et al.*, 2002; Woodman and Futter, 2008; Raiborg and Stenmark, 2009). This process is crucial for determining the amplitude of growth factor signaling and is therefore tightly regulated. The complete journey of epidermal growth factor (EGF)-activated EGF receptor (EGFR) from the cell surface to the degradative lysosome near the cell center has been described (Dikic, 2003; Miaczynska *et al.*, 2004; Citri and Yarden, 2006; Madshus and Stang, 2009; Sorkin and Goh, 2009; Sorkin and von Zastrow, 2009). Activated EGF receptors are first internalized through clathrin-dependent endocytosis. The receptors are then either sorted into recycling endosomes, which return them to the cytoplasmic membrane, or are trafficked through a series of endocytic compartments where they are sorted for proteolytic degradation in the lysosome (Maxfield and McGraw, 2004; Soldati and Schliwa, 2006; Mukhopadhyay and Riezman, 2007; Woodman and Futter, 2008). The lysosomal degradation of EGFR requires maturation of the endosomes from early to late, during which time the endosomes move along microtubules toward the cell center. During the maturation of endosomes, EGFR is sorted into the intraluminal vesicles of morphologically distinctive endosomes known as multivesicular bodies (MVBs; Katzmann *et al.*, 2002; Williams and Urbe, 2007; Hurley, 2008; Woodman and Futter, 2008; Henne *et al.*, 2011). These mature MVBs/late endosomes fuse with lysosomes, resulting in EGFR degradation. Thus endosomal trafficking of EGFR is crucial for determining the amplitude and duration of EGFR signaling. Deregulation of this pathway has been linked to the development

This article was published online ahead of print in MBoC in Press (http://www.molbiolcell.org/cgi/doi/10.1091/mbc.E11-09-0780) on February 15, 2012.

K.I., H.H., and K.M. designed the study and collected and analyzed the data. K.I. performed the experiments, except for that reported in Figure 1B. H.H. carried out the work reported in Figure 1B, and A.N. performed the electron microscopy analysis. K.I., H.H., and K.M. wrote and edited the manuscript. All of the authors discussed the results and commented on the manuscript.

The authors declare that they have no conflict of interest.

Address correspondence to: Kunihiro Matsumoto (g44177a@nucc.cc.nagoya-u.ac.jp).

Abbreviations used: CI-MPR, cation-independent mannose 6-phosphate receptor; COR, C-terminal of ROC; EEA1, early endosomal antigen 1; EGFR, epidermal growth factor receptor; ERC, endocytic recycling compartment; ESCRT, endosomal sorting complex required for transport; LAMP1, lysosomal-associated membrane protein 1; LBPA, lysobiophosphatidic acid; LRRK1, leucine-rich repeat kinase 1; MVB, multivesicular body; Rh, rhodamine; ROC, Ras of complex proteins; Tf, transferrin; WT, wild type.

and progression of various types of human cancers (Polo *et al.*, 2004; Hynes and Lane, 2005; Sharma *et al.*, 2007). In spite of considerable effort researching EGFR intracellular transport, the detailed mechanisms underlying endosomal trafficking of EGFR are not well understood.

We recently reported that leucine-rich repeat kinase 1 (LRRK1) is involved in the trafficking of activated EGFR, specifically in the progression from early to late endosomes (Hanafusa *et al.*, 2011). LRRK1 belongs to the ROCO family of proteins and contains a Ras of complex proteins (ROC) GTPase domain, a C-terminal of ROC (COR) domain, a MAPKKK-like kinase domain, and several protein–protein interaction domains (Bosgraaf and Van Haastert, 2003). The N-terminus of LRRK1 interacts with Grb2, an adaptor protein for EGFR, and LRRK1 forms a complex with EGFR via Grb2 in response to EGF stimulation. Subsequently, the LRRK1/EGFR complex is internalized and localized in early endosomes, where LRRK1 regulates the transition of EGFR from early to late endosomes in a manner dependent on its kinase activity. Although the kinase activity of LRRK1 plays an important role in EGFR trafficking, it is unclear how LRRK1 kinase activity is regulated in this process.

In this study, we show that LRRK1 is a substrate for the EGFR tyrosine kinase. On EGF stimulation, LRRK1 becomes phosphorylated at Tyr-944, resulting in inactivation of its kinase activity. The nonphosphorylated LRRK1(Y944F) mutation exhibits hyperactivation of kinase activity and enhances the motility of EGF-containing endosomes, leading to EGFR accumulation in mixed endosomes in the perinuclear region. Our results suggest that the EGFR-mediated tyrosine phosphorylation of LRRK1 plays an important role in the proper endosomal trafficking of EGFR.

RESULTS

LRRK1 is phosphorylated at the Tyr-944 residue in response to EGF stimulation

We recently showed that LRRK1 forms a complex with activated EGFR through a mutual interaction with Grb2 (Hanafusa *et al.*, 2011). We further observed that LRRK1 was phosphorylated at tyrosine residues in response to EGF stimulation. To further examine this phosphorylation, Cos7 cells were transfected with green fluorescent protein (GFP)–tagged LRRK1 (Figure 1A) and stimulated with EGF. Cell extracts were subjected to immunoprecipitation with anti-GFP antibody, followed by immunoblotting with anti-phosphotyrosine (pY) antibody. These immunoblots confirmed that LRRK1 was phosphorylated at tyrosine residues in a manner dependent on EGF stimulation (Figure 1B, lanes 1 and 2). EGFR was coimmunoprecipitated with LRRK1 and was tyrosine phosphorylated in cells stimulated by EGF (Figure 1B, lanes 1 and 2).

To determine which region of LRRK1 is tyrosine phosphorylated, we generated several deletion mutants of LRRK1 (Figure 1A). Consistent with our previous results (Hanafusa *et al.*, 2011), the C-terminal–deleted mutants LRRK1-N1 and -N2 were able to associate with activated EGFR in response to EGF stimulation (Figure 1B, lanes 3–6). We found that the LRRK1-N1 fragment was tyrosine phosphorylated after EGF stimulation (Figure 1B, lanes 3 and 4), whereas LRRK1-N2 lacking the ROC-COR domain was only weakly tyrosine phosphorylated (Figure 1B, lane 6). In contrast, the N-terminal–deleted mutants LRRK1-C1 and -C2 were unable to associate with EGFR and were not tyrosine phosphorylated (Figure 1B, lanes 7–10). These results suggest that EGFR or an EGFR-associated tyrosine kinase phosphorylates LRRK1 primarily in the ROC-COR domain in a manner dependent on its association with EGFR. Therefore we asked whether LRRK1 is a substrate for EGFR. The in vitro tyrosine phosphorylation of immunopurified GFP-LRRK1 was examined in the presence or absence of active recombinant EGFR protein. We detected tyrosine-phosphorylated LRRK1 only in the presence of EGFR (Figure 1C), indicating that LRRK1 may be a substrate for EGFR.

Next we attempted to identify the sites in LRRK1 that are tyrosine phosphorylated in an EGFR-dependent manner. The ROC-COR domain of LRRK1 contains one EGFR tyrosine kinase consensus site (Glu-Glu-Glu-Tyr-Phe) at residue 944 (Figure 1A; Ubersax and Ferrell, 2007). To examine whether this site is responsible for EGFR-mediated tyrosine phosphorylation, we generated a polyclonal antibody directed against a peptide encompassing phospho–Tyr-944 (pY944). Cos7 cells were transfected with GFP-LRRK1 and stimulated with the EGF ligand. We immunoprecipitated GFP-LRRK1 with anti-GFP antibody and probed the blots with anti-pY944 antibody. Phosphorylation of LRRK1 Tyr-944 was detected upon EGF stimulation, and this phosphorylation was enhanced by the treatment with the tyrosine phosphatase inhibitor vanadate (Figure 1D, lanes 1–4). To confirm that EGF stimulation induces LRRK1 Y944 phosphorylation, we constructed the Y944F mutation in which Tyr-944 has been mutated to Phe. When cells were stimulated with EGF in the presence of vanadate, LRRK1(Y944F) was not recognized by the anti-pY944 LRRK1 antibody (Figure 1D, lane 6). This mutant construct also provided a control for the pY944-specific LRRK1 antibody.

The foregoing results indicate that LRRK1 Y944 phosphorylation is modulated by EGFR activation. We next determined whether endogenous LRRK1 is phosphorylated at Tyr-944 in response to EGF stimulation. Cos7 cells were stimulated with EGF, and endogenous LRRK1 was examined by immunoblotting with anti-pY944 LRRK1 antibody. We observed that LRRK1 Tyr-944 was phosphorylated following EGF stimulation (Figure 1E). Taken together, these results suggest that LRRK1 associates with EGFR and is phosphorylated at the Tyr-944 residue in response to EGF stimulation.

Phosphorylation of LRRK1 at Tyr-944 negatively regulates its kinase activity

The Tyr-944 residue is located in the COR domain between the ROC GTPase and kinase domains (Figure 1A). Because phosphorylation represents an important posttranslational modification that regulates GTP-binding and kinase activities, we examined the effect of the nonphosphorylatable LRRK1(Y944F) mutation on these activities. Cos7 cells were transfected with GFP-LRRK1, and LRRK1 proteins were subsequently assayed for GTP-binding activity. We found that the LRRK1(Y944F) mutant showed higher levels of GTP binding compared with wild-type LRRK1 (Figure 2A, lanes 2 and 3). This suggests that phosphorylation at Tyr-944 negatively regulates the GTP-binding activity of LRRK1. Consistent with this, amino acid substitutions that mimic phosphorylation at Tyr-944 (Y944E and Y944D) abrogated GTP binding, similar to the LRRK1(S625N) mutant lacking the GTP-binding activity (Hanafusa *et al.*, 2011; Figure 2A, lanes 4, 6, and 7).

To examine the effect of the LRRK1(Y944F) mutation on LRRK1 kinase activity, immunoprecipitated LRRK1 proteins were assayed for autophosphorylation activity. Compared to wild-type LRRK1 (Figure 2B, lane 1), LRRK1(Y944F) showed much higher autophosphorylation activity (Figure 2B, lane 3). This activity was solely due to immunoprecipitated LRRK1(Y944F), since no phosphorylation was observed in immunoprecipitates from cells expressing the double mutant LRRK1(Y944F; K1243M), which also carries the kinase-deficient K1243M mutation (Figure 2B, lane 4). Furthermore, the phosphomimic mutations LRRK1(Y944E) and LRRK1(Y944D) abrogated autophosphorylation activity, similar to

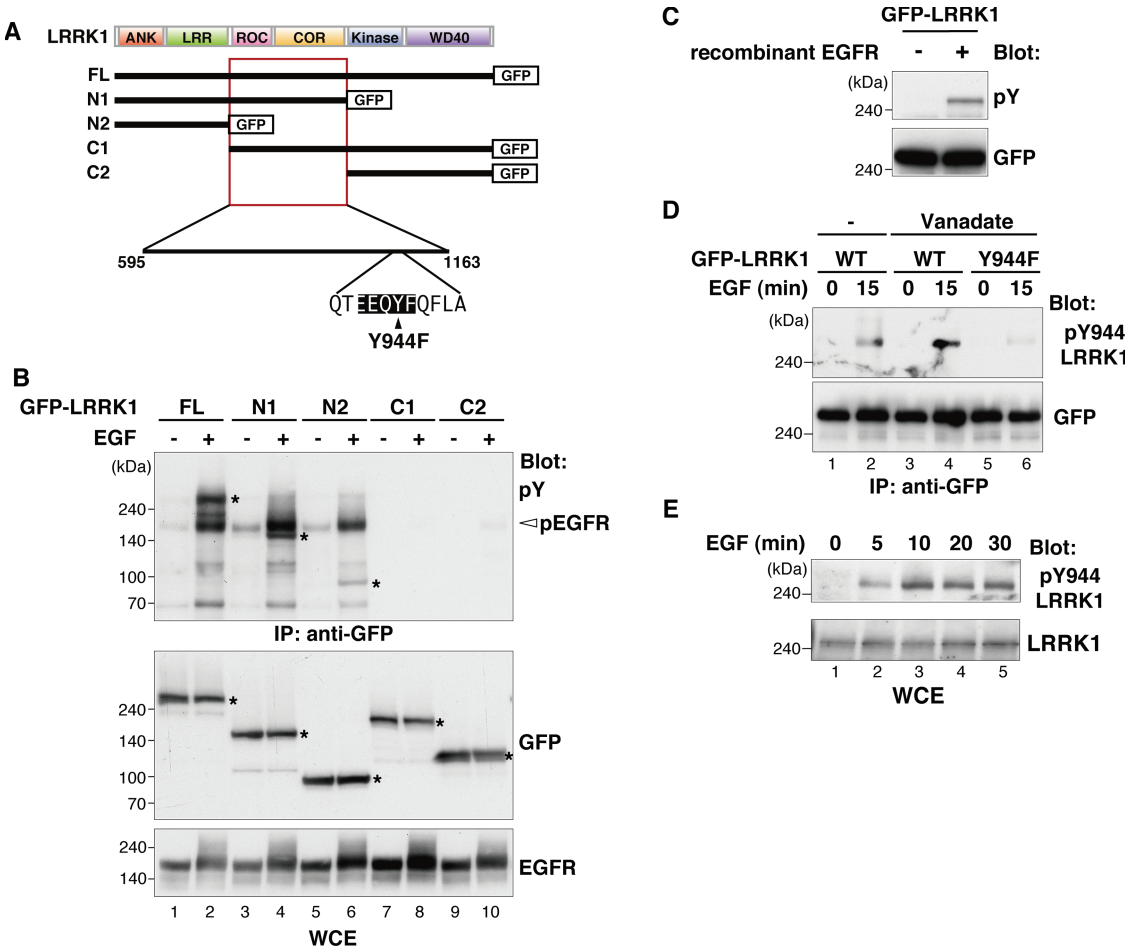

FIGURE 1: LRRK1 is phosphorylated at Tyr-944 residue in response to EGF stimulation. (A) Schematic diagram of human LRRK1. Domains are as follows: leucine-rich repeats (LRR), a ROC domain, a COR domain, a MAPKKK-like kinase domain, and WD40 repeats. Deletion constructs of LRRK1 are shown below. The arrowhead indicates the amino acid substitution used in this study. (B) LRRK1 is tyrosine phosphorylated in the ROC-COR domain upon EGF stimulation. Cos7 cells were transfected with GFP-tagged, full-length (FL) LRRK1 and deletion mutants, as indicated. After 16 h of serum starvation, cells were stimulated with EGF (100 ng/ml) for 15 min. Whole-cell extracts (WCEs) and immunoprecipitated complexes obtained with anti-GFP antibody (IP: anti-GFP) were immunoblotted with the indicated antibodies. Asterisks indicate the positions of LRRK1. (C) Recombinant EGFR phosphorylates tyrosine residues on LRRK1 in vitro. Cos7 cells were transfected with GFP-LRRK1, and cell lysates were immunoprecipitated with anti-GFP antibody. The immunopurified LRRK1 proteins were subjected to in vitro kinase assay using recombinant human EGFR protein. Phosphorylated LRRK1 was detected by immunoblotting with anti-pY antibody. Equal protein input was confirmed by immunoblotting with anti-GFP antibody. (D) LRRK1 Tyr-944 residue is phosphorylated in response to EGF stimulation. Cos7 cells were transfected with wild-type (WT) GFP-LRRK1 and GFP-LRRK1(Y944F), as indicated. Cells were stimulated with EGF (100 ng/ml) for 15 min with or without vanadate pretreatment. Experiments were carried out as in B, with immunoblotting by the appropriate antibodies. (E) Endogenous LRRK1 is phosphorylated at Tyr-944 in response to EGF stimulation. Cos7 cells were stimulated with EGF (100 ng/ml) for the indicated times, and cell lysates were examined for immunoblotting with the indicated antibodies.

the kinase-inactive LRRK1(K1243M) mutant (Figure 2B, lanes 2, 5, and 6). It was reported that LRRK1 kinase activity is activated by binding of GTP in the ROC GTPase domain (Korr *et al.*, 2006). To examine whether the stimulation of LRRK1 kinase activity by the Y944F mutation is dependent on the GTP-bound state, we constructed the double mutant containing Y944F and S625N. As observed previously (Hanafusa *et al.*, 2011), the LRRK1(S625N) mutant lacked kinase activity (Figure 2B, lane 8). Similarly, the LRRK1(Y944F; S625N) mutant was unable to bind to GTP-agarose (Figure 2A, lane 5). Of importance, LRRK1(Y944F; S625N) could no longer autophosphorylate (Figure 2B, lane 10). Taken together, these results suggest that phosphorylation of LRRK1 at Tyr-944 causes the accumulation of the GDP-bound state, thereby inhibiting LRRK1 kinase activity.

We next examined the effect of EGF stimulation on LRRK1 kinase activity. Cos7 cells were transfected with wild-type GFP-LRRK1 and then treated with EGF for various times. LRRK1 proteins were immunoprecipitated and assayed for autophosphorylation activity. LRRK1 kinase activity was transiently activated by EGF stimulation, peaked at 10 min, and then declined (Figure 2C, lanes 1–6). In contrast, the kinase activity of the LRRK1(Y944F) mutant was more enhanced and was sustained for up to 120 min after EGF stimulation (Figure 2C, lanes 7–16). No autophosphorylation was observed in immunoprecipitates of the LRRK1(Y944F; K1243M) mutant, similar

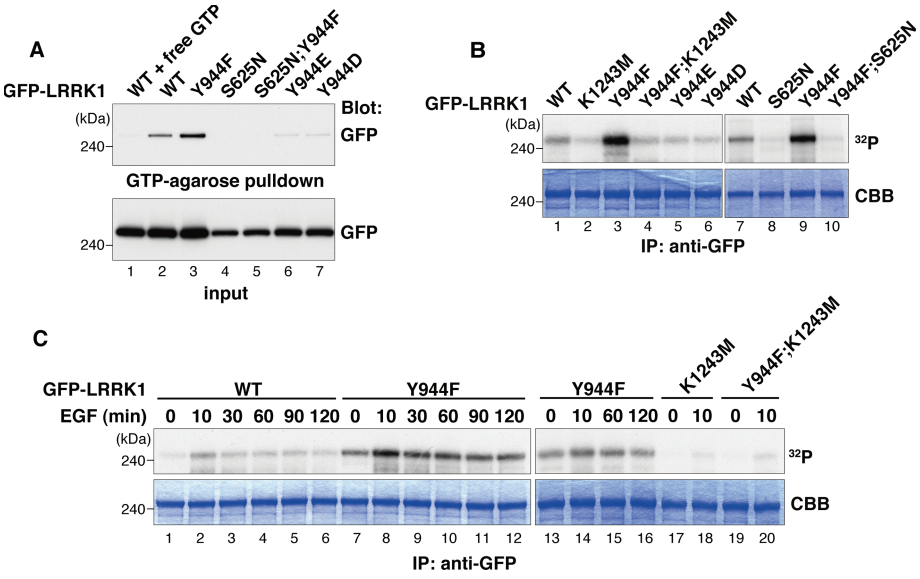

FIGURE 2: Phosphorylation of LRRK1 at Tyr-944 reduces its kinase activity. (A) GTP-binding activity of LRRK1 mutants. Cos7 cells were transfected with WT GFP-LRRK1, GFP-LRRK1(Y944F), GFP-LRRK1(S625N), GFP-LRRK1(Y944F; S625N), GFP-LRRK1(Y944E), and GFP-LRRK1(Y944D), as indicated. Using GTP-agarose, GFP-LRRK1 protein was affinity purified from cytosolic extracts of transfected Cos7 cells in the presence or absence of 4 mM GTP (top). Protein input was confirmed by immunoblotting with anti-GFP antibodies (bottom). (B) Kinase activity of LRRK1 mutants. Cos7 cells were transfected with WT and LRRK1 mutants, as indicated. Immunoprecipitated samples were incubated with [γ-^{32}P]ATP for 20 min at 30°C. Autophosphorylated LRRK1 was resolved by SDS–PAGE and stained with Coomassie blue to visualize total amounts of precipitated LRRK1 proteins. (C) The effect of EGF stimulation on LRRK1 kinase activity. Cos7 cells were transfected with WT GFP-LRRK1 and LRRK1 mutants, as indicated. After 16 h of serum starvation, cells were stimulated with EGF (100 ng/ml) for the indicated times. In vitro autophosphorylation assays were carried out as in B.

to LRRK1(K1243M) (Figure 2C, lanes 17–20). Thus kinase activity correlates with autophosphorylation activity in immunoprecipitated LRRK1(Y944F). These results suggest that LRRK1 is activated in response to EGF stimulation and subsequently inactivated by EGFR-mediated Tyr-944 phosphorylation in a negative feedback manner.

LRRK1 kinase activity regulates the motility of EGF-containing endosomes

Because the kinase activity of LRRK1 is required for motility of EGF-containing endosomes (Hanafusa *et al.*, 2011), we examined the effect of LRRK1 hyperactivation on the dynamics of EGF movement in vivo using time-lapse confocal fluorescence microscopy. The movement of EGF-containing endosomes was followed in HeLa cells expressing GFP-LRRK1 at 15 min after a brief pulse of fluorescent EGF (Alexa 647-EGF). Under these conditions, the fluorescence detected in cells was due to endocytosed EGFR bound to labeled growth factor. Most of the internalized Alexa 647-EGF colocalized with GFP-LRRK1 (Figure 3, A–C, and Supplemental Figure S1, A–C). In addition to short-range movement, long-range rapid movement of GFP-LRRK1 and Alexa 647-EGF double-positive endosomes was frequently observed (Figure 3, A and D). When HeLa cells were transfected with GFP-LRRK1(Y944F) and treated with Alexa 647-EGF, the frequency of EGF long-range movement was remarkably increased (Figure 3, B and D). In contrast, EGF long-range movement was decreased in cells expressing the kinase-inactive LRRK1(Y944F; K1243M) (Figure 3, C and D). In cells expressing wild-type LRRK1, 17.4% of endosomes containing both GFP-LRRK1 and Alexa 647-EGF moved >5.0 µm during the imaging time (35 s). This fraction increased to 34.7% in LRRK1(Y944F)-expressing cells and decreased to 6.8% in cells expressing LRRK1(Y944F; K1243M) (Figure 3E). These results suggest that hyperactivation of LRRK1 kinase activity enhances the long-range rapid movement of EGF-containing endosomes.

Hyperactivation of LRRK1 causes EGF/EGFR accumulation in perinuclear endosomes

Next we investigated the effect of the LRRK1(Y944F) mutation on the intracellular distribution of EGF/EGFR after EGF stimulation. We expressed GFP-LRRK1 in HeLa S3 cells and assessed EGF localization by immunofluorescence using a fluorescently labeled rhodamine-conjugated EGF (Rh-EGF). Cells expressing wild-type GFP-LRRK1 were briefly stimulated with Rh-EGF. By 10 min poststimulation, Rh-EGF was distributed in a fine, punctate pattern that colocalized with GFP-LRRK1 (Figure 4, A and E). After 30 min, weak punctate staining of Rh-EGF was colocalized with GFP-LRRK1 in the perinuclear region, suggesting that transport of EGF/EGFR from early to late endosomes. After 60 min, most of the Rh-EGF signal had disappeared and GFP-LRRK1 was diffusely distributed, suggesting that EGF/EGFR had been degraded in lysosomes and/or recycled.

In GFP-LRRK1(Y944F)–expressing cells briefly stimulated with EGF, the distribution of Rh-EGF at 10 min was similar to that observed in cells expressing wild-type LRRK1 (Figure 4, B and E). However, at 30 min, both Rh-EGF and GFP-LRRK1(Y944F) had accumulated in compartments in the perinuclear area and remained there up to 60 min after EGF stimulation. Thus EGFR degradation appears to be impaired in these cells. In contrast, expression of the kinase-inactive GFP-LRRK1(Y944F; K1243M) failed to induce accumulation of Rh-EGF in the perinuclear region (Figure 4C and E), suggesting that the phenotype associated with LRRK1(Y944F) is caused by hyperactivation of LRRK1 kinase activity. Similar results were observed by immunofluorescent staining with anti-EGFR antibodies in HeLa S3 cells expressing wild-type GFP-LRRK1 or LRRK1(Y944F) (Supplemental Figure S2). Thus expression of LRRK1(Y944F) leads to the accumulation of EGF/EGFR in perinuclear endosomes and the delay of EGFR degradation/recycling.

We also considered the possibility that the observed effects of LRRK1(Y944F) might be due to secondary effects caused by its overexpression. To exclude this possibility, we depleted endogenous LRRK1 using small interfering RNA (siRNA) in HeLa S3 cells and expressed siRNA-resistant versions of wild-type LRRK1, LRRK1(Y944F), or LRRK1(Y944F; K1243M) at levels similar to those of endogenous LRRK1 (Supplemental Figure S3A). In LRRK1-depleted cells expressing siRNA-resistant wild-type GFP-LRRK1, weak punctate staining of Rh-EGF colocalized with GFP-LRRK1 in the perinuclear region at 30 min after Rh-EGF stimulation (Supplemental Figure S3, B and E). When siRNA-resistant GFP-LRRK1(Y944F) was reintroduced into LRRK1-depleted cells, both Rh-EGF and GFP-LRRK1(Y944F) accumulated in compartments in the perinuclear area by 30 min poststimulation (Supplemental Figure S3, C and E). Furthermore, we found that expression of siRNA-resistant GFP-LRRK1(Y944F;

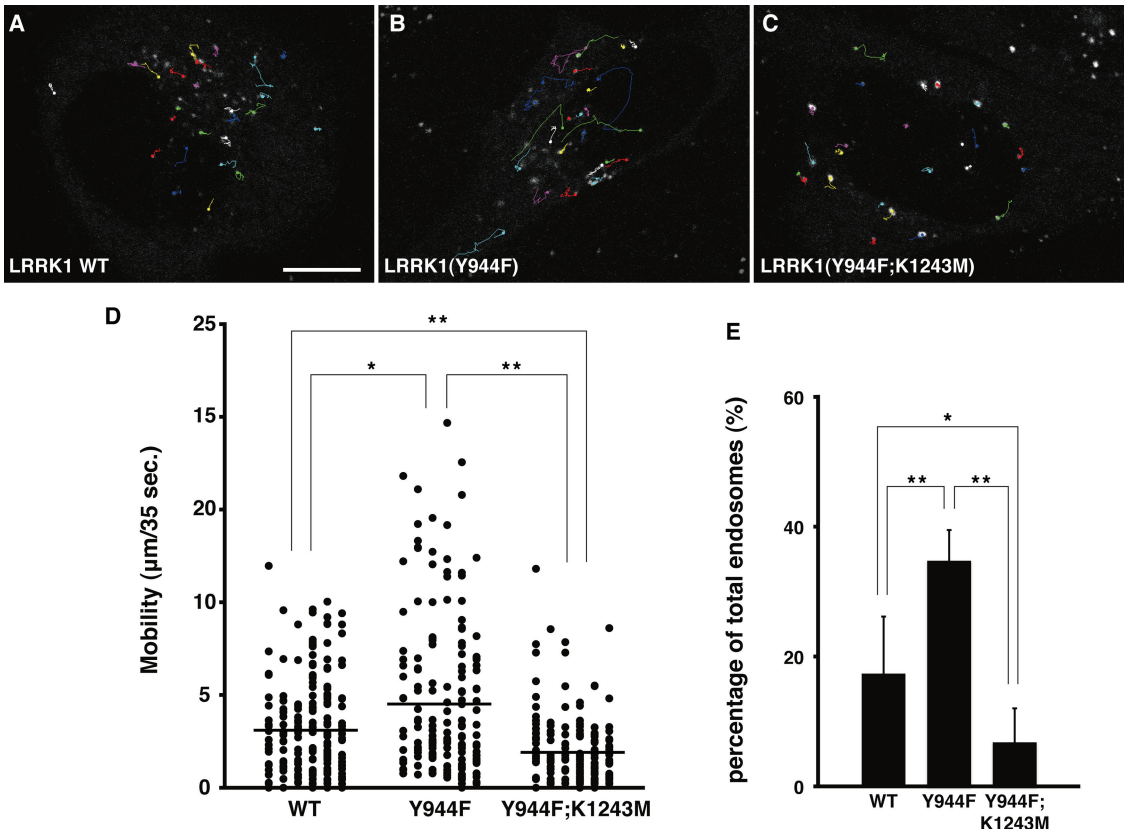

FIGURE 3: LRRK1(Y944F) promotes the motility of EGF-containing endosomes. (A–C) Images representing Alexa 647-EGF and GFP-LRRK1double-positive endosomes (circles) and tracks (lines). HeLa S3 cells were transfected with WT GFP-LRRK1 (A), GFP-LRRK1(Y944F) (B), and GFP-LRRK1(Y944F; K1243M) (C) and pulse labeled with Alexa 647-EGF for 3 min. Movement of EGF/LRRK1–containing endosomes were observed by time-lapse confocal fluorescence microscopy and analyzed using the Manual Tracking ImageJ plug-in. Imaging started at 15 min after the initial exposure to Alexa 647-EGF, with frames captured at 1.165-s intervals for 35 s. Scale bar, 10 μm. (D) A mobility dot plot of the Alexa 647-EGF and GFP-LRRK1 double-positive endosomes. Mobility is defined as the distance of the trajectory of endosomes ($n > 150$) during the 35-s observation periods, quantified using the Manual Tracking ImageJ plug-in. The data are combined from six independent experiments and compared by the Mann–Whitney U test. *$p < 0.05$; **$p < 0.01$. The horizontal bars indicate the mean of total endosomes. (E) Quantification of long-range movement (>5.0 μm) of Alexa 647-EGF and GFP-LRRK1 double-positive endosomes. Values reflect the mean SD of six independent experiments, with an average of 30 EGF/LRRK1–containing endosomes scored per experiment. Data are compared using a two-tailed unpaired Student's *t* test. *$p < 0.05$; **$p < 0.01$.

K1232M) in LRRK1-depleted cells failed to induce accumulation of Rh-EGF in the perinuclear region (Supplemental Figure S3, D and E). These results suggest that the kinase function of LRRK1 is important for the proper endosomal trafficking of EGF/EGFR.

Because the movement of endosomes from the cell periphery to the cell center depends on motor protein–mediated transport along microtubules, we determined whether intact microtubules are required for the LRRK1(Y944F)-induced accumulation of EGF in the perinuclear region. We treated cells expressing LRRK1(Y944F) with nocodazole, a microtubule-depolymerizing agent, prior to EGF stimulation. In the presence of nocodazole, fluorescent punctae were widely dispersed throughout the cell (Figure 4, D and E). These results suggest that hyperactivation of LRRK1 causes the accumulation of EGF/EGFR in perinuclear endosomes through microtubule-mediated transport.

LRRK1(Y944F) induces the formation of EGF-containing mixed endosomes

We investigated the characteristics of the LRRK1(Y944F)-induced perinuclear endosomes using early endosomal antigen 1 (EEA1) and cation-independent mannose 6-phosphate receptor (CI-MPR) as early and late endosomal markers, respectively. Cells expressing wild-type GFP-LRRK1 were briefly stimulated with Rh-EGF. After 30 min, very little of the Rh-EGF was colocalized with EEA1 (Figure 5A) and some of them colocalized with CI-MPR in the juxtanuclear area (Figure 5B). In contrast, when GFP-LRRK1(Y944F)–expressing cells were stimulated with Rh-EGF, the ligand was found 30 min later to have accumulated in perinuclear compartments positive for both EEA1 and CI-MPR (Figure 5, D and E). To confirm that LRRK1(Y944F) induced colocalization of EEA1 and CI-MPR to the same compartment rather than in distinct compartments that have coalesced, we examined localization by immuno–electron microscopy. We stimulated wild-type GFP-LRRK1– or GFP-LRRK1(Y944F)–expressing cells with EGF and analyzed the localization of endogenous EEA1 and CI-MPR by immunostaining with gold particles of different sizes. At 30 min after EGF stimulation, endogenous EEA1 and CI-MPR were localized in distinct compartments in cells expressing wild-type GFP-LRRK1 (Supplemental Figure S4, A and B). In contrast, in GFP-LRRK1(Y944F)–expressing cells, EEA1 and CI-MPR were localized in the same

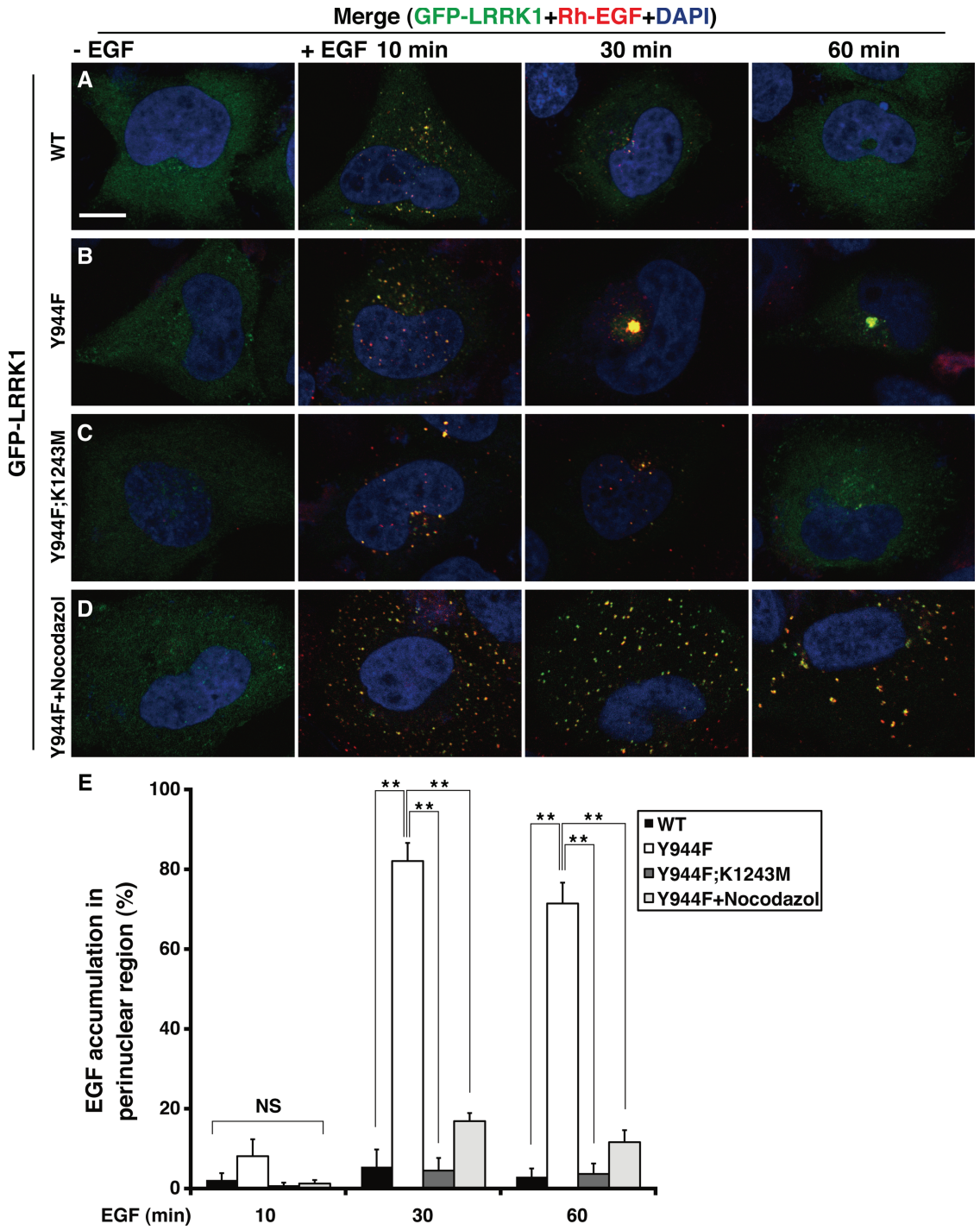

FIGURE 4: LRRK1(Y944F) leads to EGF accumulation in endosomal compartments in the perinuclear region. (A–D) Distribution of Rh-EGF. HeLa S3 cells were transfected with wild-type GFP-LRRK1 (A), GFP-LRRK1(Y944F) (B, D), and GFP-LRRK1(Y944F; K1243M) (C), as indicated. After 16 h of serum starvation, cells were briefly stimulated with or without Rh-EGF (40 ng/ml), followed by washing to remove labeled EGF from the medium. The cells shown in D were preincubated with nocodazole (5 μg/ml) for 30 min before EGF stimulation. Cells were incubated for the indicated times after the initial exposure to Rh-EGF and then fixed and stained with 4′,6-diamidino-2-phenylindole. Yellow colors in the merged images indicate colocalization of GFP-LRRK1 and Rh-EGF. Scale bar, 10 μm. (E) Quantification of the EGF accumulation in the perinuclear region. Histogram indicates the percentage of cells that have endosomes (>2.0 μm diameter) containing Rh-EGF in the perinuclear region. Values reflect the mean SD of three independent experiments, with an average of 50 cells scored per samples. Data are compared using a two-tailed unpaired Student's *t* test. *$p < 0.05$; **$p < 0.01$; NS, not significant.

compartment (Supplemental Figure S4C). Thus we conclude that the LRRK1(Y944F) mutation induces the formation of compartments containing both EEA1 and CI-MPR.

Next we examined the effect of LRRK1(Y944F) on the recycling pathway. We followed this pathway using fluorescent Alexa 647–transferrin (Alexa 647-Tf), since transferrin is known to be

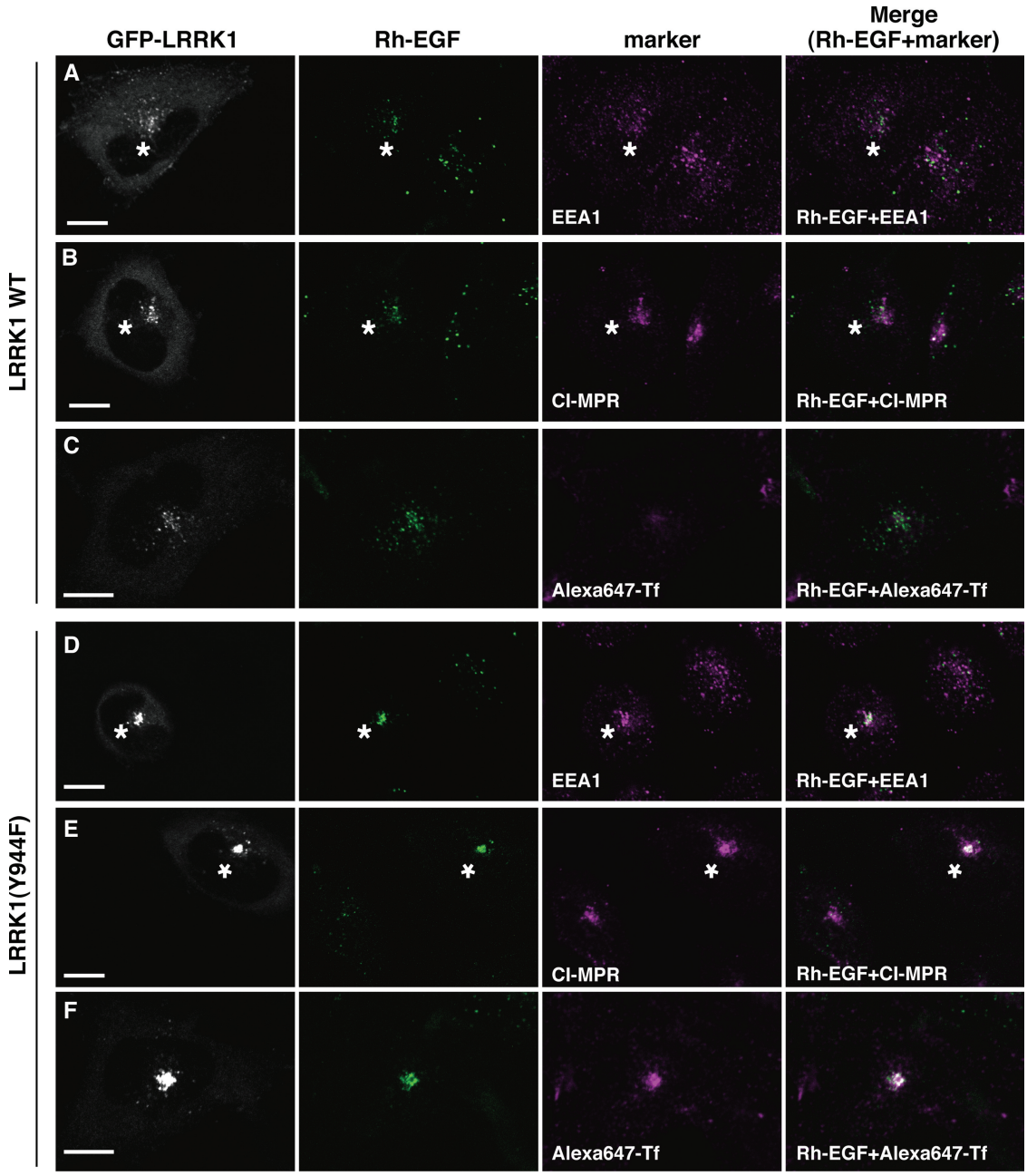

FIGURE 5: LRRK1(Y944F) induces the formation of mixed endosomes. HeLa S3 cells were transfected with WT GFP-LRRK1 (A–C) and GFP-LRRK1(Y944F) (D–F), as indicated. After 16 h of serum starvation, cells were briefly stimulated with Rh-EGF (40 ng/ml), followed by washing to remove labeled EGF from the medium. The cells were incubated for 30 min after the initial exposure to Rh-EGF and immunostained with anti-EEA1 (A, D) and anti–CI-MPR (B, E) antibodies. For Tf recycling (C, F), cells were briefly treated with Rh-EGF and Alexa 647-Tf (5 μg/ml), followed by washing to remove labeled EGF and Tf from the medium. The cells were incubated with unlabeled Tf (60 μg/ml) for 30 min after the initial exposure to Rh-EGF and Alexa 647-Tf and fixed. Asterisks indicate cells expressing wild-type GFP-LRRK1 (A, B) and GFP-LRRK1(Y944F) (D, E), respectively. Scale bars, 10 μm.

recycled from the peripheral early endosome back to the cell surface either by rapid recycling endosomes or the juxtanuclear endocytic recycling compartment (ERC; Sonnichsen *et al.*, 2000; De Domenico *et al.*, 2008; Grant and Donaldson, 2009). When wild-type GFP-LRRK1–expressing cells were briefly stimulated with Alexa 647-Tf in the absence of EGF, punctate fluorescence at both the periphery and perinuclear region were observed at 10 min (Supplemental Figure S5A). A significant amount of Tf localized to the juxtanuclear ERC by 20 min (Supplemental Figure S5B). After 30 min, Alexa 647-Tf fluorescence disappeared (Supplemental Figure S5C), suggesting that the labeled transferrin had recycled back to the plasma membrane. In the absence of EGF stimulation, localization of Alexa 647-Tf appeared similar regardless of whether wild-type GFP-LRRK1 or GFP-LRRK1(Y944F) was expressed in the cell (Supplemental Figure S5). Under these conditions, GFP-LRRK1 and GFP-LRRK1(Y944F) were diffusely distributed.

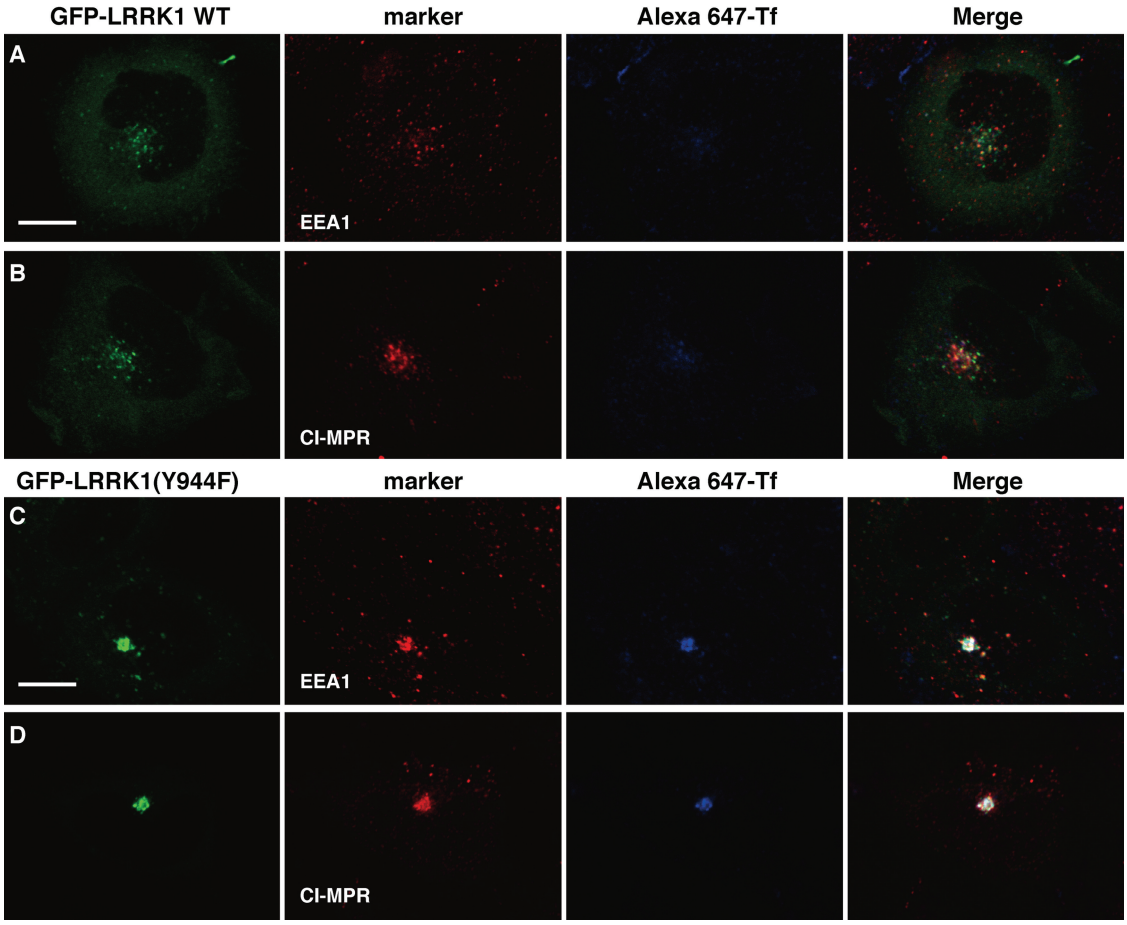

FIGURE 6: LRRK1 (Y944F) induces Tf accumulation in EEA1and CI-MPR double-positive endosomes. HeLa S3 cells were transfected with WT GFP-LRRK1 (A, B) and GFP-LRRK1(Y944F) (C, D), as indicated. After 16 h of serum starvation, cells were briefly stimulated with EGF (50 ng/ml) and Alexa 647-Tf (5 µg/ml), followed by washing to remove them from medium. Then cells were incubated with unlabeled Tf (60 µg/ml) and fixed at 30 min after the initial exposure. The cells were immunostained with anti-EEA1 (A, C) and anti–CI-MPR (B, D) antibodies. Scale bars, 10 µm.

When wild-type GFP-LRRK1–expressing cells were stimulated with Rh-EGF and Alexa 647-Tf simultaneously, a large amount of Tf fluorescence was found 10 min later to colocalize in endosomes with GFP-LRRK1 and Rh-EGF (Supplemental Figure S6A). After 20 min, most of the Alexa 647-Tf disappeared from endosomes containing GFP-LRRK1 and Rh-EGF and relocalized to the juxtanuclear ERC (Supplemental Figure S6B). At 30 min, little or no Alexa 647-Tf fluorescence was observed, indicating that it had recycled back to the cell surface, whereas GFP-LRRK1 and Rh-EGF fluorescence was detected in the perinuclear region (Figure 5C and Supplemental Figure S6C). Expression of LRRK1(Y944F) had no effect on the uptake or initial localization of Alexa 647-Tf at 10 min after stimulation with Rh-EGF and Alexa 647-Tf (Supplemental Figure S6D). However, after 20–30 min, Alexa 647-Tf remained associated in endosomes with GFP-LRRK1(Y944F) and Rh-EGF and accumulated in juxtanuclear endosomes (Figure 5F and Supplemental Figure S6, E and F). These results suggest that expression of LRRK1(Y944F) perturbs the recycling of Tf back to the cell surface from endosomes, leading to accumulation of Tf in the juxtanuclear endosomes, in a manner dependent on EGF stimulation. Furthermore, we found that expression of LRRK1(Y944F), but not wild-type LRRK1, induced the colocalization of Alexa 647-Tf with EEA1 and CI-MPR in the endosome at 30 min after stimulation with EGF and Alexa 647-Tf (Figure 6). On the other hand, these compartments did not contain markers for late endolysosomal compartments, such as lysobiophosphatidic acid (LBPA) or lysosomal-associated membrane protein 1 (LAMP1; Figure 7, A and B), or those for Golgi network, such as GM130 (a *cis*-Golgi marker) or p230 (a *trans*-Golgi marker) (Figure 7, C and D). Taken together, these results suggest that LRRK1(Y944F) induces the accumulation of endocytic membrane in the perinuclear region from which both recycling and degradative cargo are unable to escape.

Hyperactivation of LRRK1 fails to form proper intraluminal vesicles of MVBs

We next used electron microscopy to more closely examine the effect of LRRK1(Y944F) on the nature and morphology of EGF/EGFR–containing endosomes. We stimulated control or GFP-LRRK1–expressing cells with EGF and analyzed the localization of endogenous EGFR by immunostaining with silver-enhanced gold particles. At 10 min after EGF stimulation, endogenous EGFR was associated with both the limiting membrane and intraluminal vesicles of MVBs in both control and wild-type GFP-LRRK1–expressing cells (Figure 8, A, B, and D). At 30 min after EGF stimulation, a large fraction of the EGFR had accumulated in lysosomes (Figure 8, E, F, and H). In contrast, in GFP-LRRK1(Y944F)–expressing cells, a significant fraction of

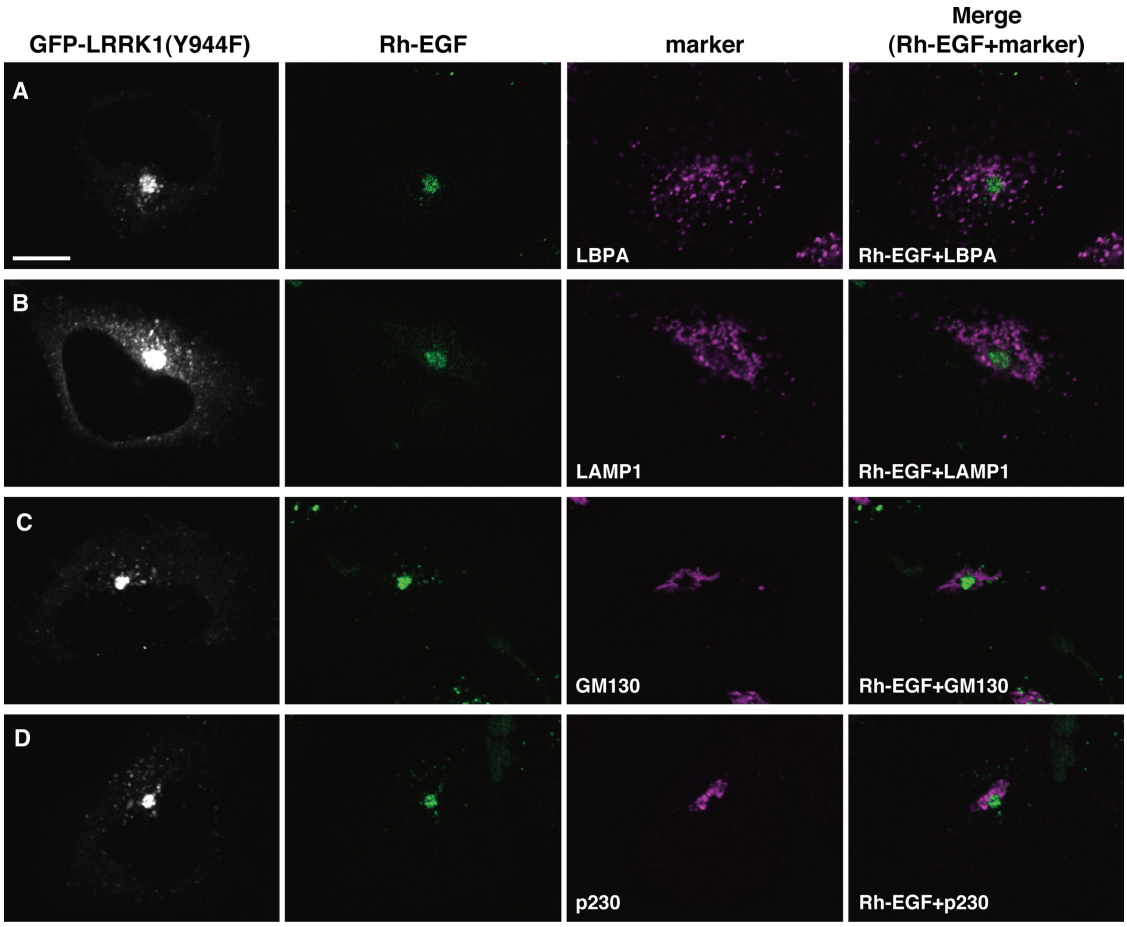

FIGURE 7: Accumulated EGF in cells expressing GFP-LRRK1 (Y944F) does not colocalize with lysosomal or Golgi markers. HeLa S3 cells were transfected GFP-LRRK1(Y944F). After 16 h of serum starvation, cells were briefly stimulated with Rh-EGF (40 ng/ml), followed by washing to remove labeled EGF from the medium. The cells were incubated for 30 min after the initial exposure to Rh-EGF and immunostained with anti-LBPA (A), anti-LAMP1 (B), anti-GM130 (C), and anti-p230 (D) antibodies. Scale bar, 10 μm.

EGFR was localized in electron-dense endosomes at 10 min after EGF stimulation (Figure 8, C and D), and a small fraction of EGFR was found in lysosomes at 30 min (Figure 8, G and H). Of note, the proper formation of intraluminal vesicles was significantly impaired in electron-dense endosomes (Figure 8C). Furthermore, in LRRK1(Y944F)-expressing cells, we observed that endosomes were morphologically abnormal, although this proportion was low, and that EGFR localized to the perinuclear region membrane (Supplemental Figure S7). These results suggest that LRRK1(Y944F) expression prevents the proper trafficking of EGFR-containing endosomes into MVBs and subsequently inhibits the delivery of EGFR to the lysosomes.

DISCUSSION

Following clathrin-mediated endocytosis, activated EGFR is delivered to the lysosome for degradation. This process is known to be regulated by the endosomal sorting complex required for transport (ESCRT) complexes (Katzmann *et al.*, 2002; Williams and Urbe, 2007; Hurley, 2008; Hurley and Hanson, 2010; Raiborg and Stenmark, 2009; Henne *et al.*, 2011). The ESCRT complexes, which are composed of ESCRT-0, -I, -II, and -III, function sequentially in sorting ubiquitinated cargoes, including EGFR, into the MVB pathway and in the formation of MVB vesicles. This transport and lysosomal degradation of activated EGFR occurs rapidly, presumably to limit excessive mitogenic EGFR signaling (Dikic, 2003; Miaczynska *et al.*, 2004; Citri and Yarden, 2006; Madshus and Stang, 2009; Sorkin and Goh, 2009; Sorkin and von Zastrow, 2009). The rapid kinetics of this process led us to postulate the existence of a more specific mechanism, in addition to the general ESCRT machinery, that regulates EGFR endosomal trafficking. However, whereas EGFR sorting to the MVB pathway by the ESCRT complexes is well established, little is understood about cargo-specific sorting. Our findings here indicate that LRRK1 kinase activity plays a role in EGFR intracellular trafficking as a cargo-specific regulator of EGFR endosomal transport.

EGFR inactivates LRRK1 kinase activity by phosphorylating Tyr-944 as a negative feedback mechanism

We previously reported that LRRK1 forms a complex with activated EGFR through an interaction with Grb2 (Hanafusa *et al.*, 2011). As a consequence, LRRK1 and EGFR are internalized and colocalized in early endosomes. LRRK1 regulates EGFR transport from early to late endosomes and regulates the motility of EGF-containing endosomes in a manner dependent on LRRK1 kinase activity. Therefore it is important to understand how LRRK1 kinase activity is regulated in the EGFR trafficking pathway. In this study, we find that LRRK1 is phosphorylated at Tyr-944 in response to EGF stimulation. LRRK1 Tyr-944 phosphorylation depends on the association with activated EGFR, and we observe in vitro that active recombinant EGFR protein

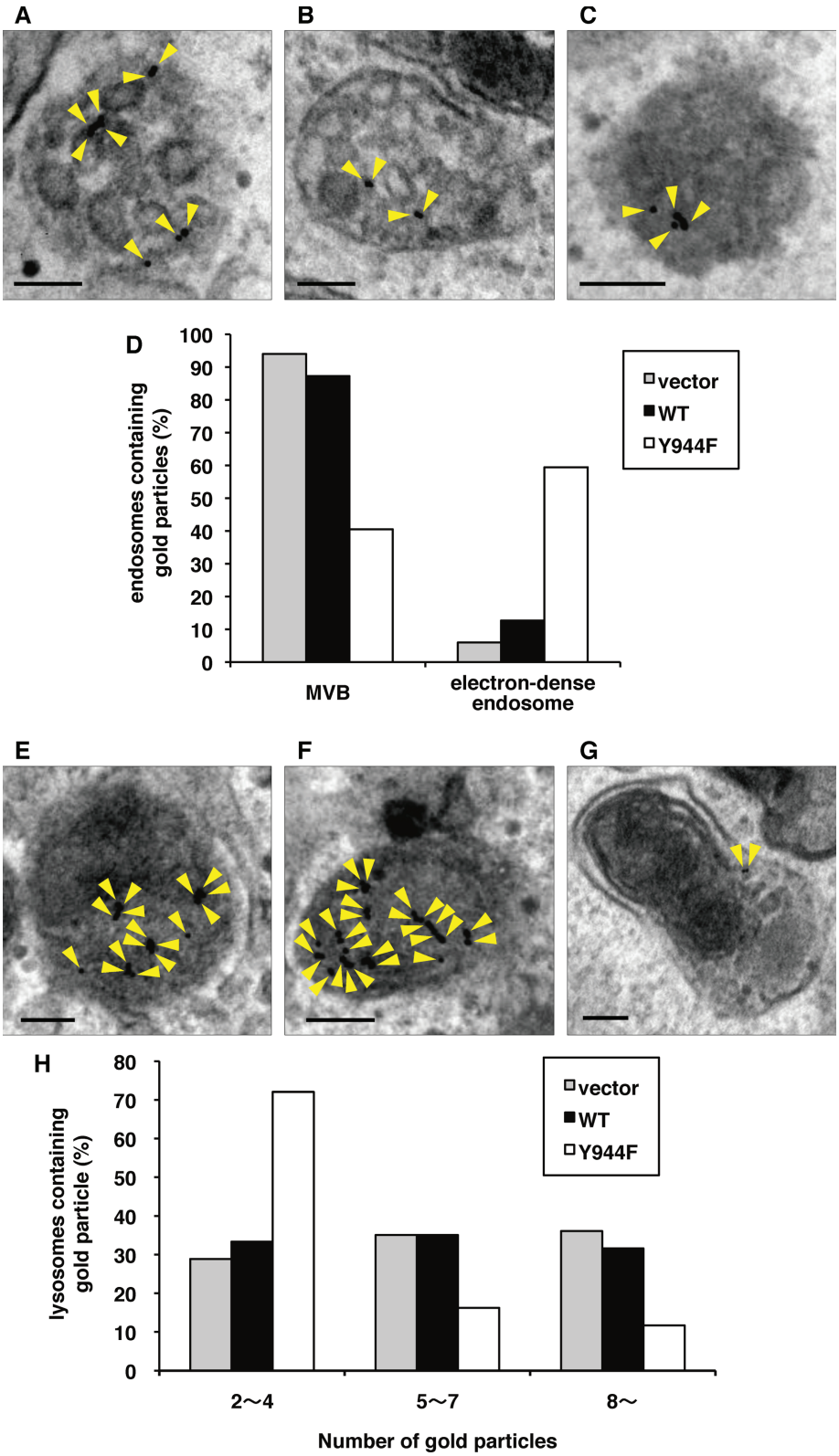

FIGURE 8: LRRK1(Y944F) fails to form proper intraluminal vesicles of MVBs. (A–C, E–G) We generated HeLa S3 cells stably expressing GFP (A, E), WT GFP-LRRK1 (B, F), and GFP-LRRK1(Y944F) (C, G) according to the manufacturer's protocol. After serum starvation, cells were incubated with anti-EGFR antibodies (LA-22) for 2 h at 37°C, followed by goat anti–mouse IgG antibodies conjugated to 10-nm gold for 1h at 37°C. After washing to remove antibodies from the medium, cells were stimulated with EGF for 10 min (A–C) and 30 min (E–G) and then fixed. The localization of EGFR was examined by conventional electron microscopy. Arrowheads indicate EGFR labeled with immunogold particles. Scale bars, 100 nm. (D) Histogram indicates the percentage of compartments (MVBs or electron-dense endosomes) containing gold particles compared with total endosomes containing gold particles after 10 min of EGF uptake. About 100 organelles that contained gold particles were counted per samples. At this time point, 64% (vector), 60% (LRRK1 WT), and 63% (LRRK1(Y944F)) of organelles were localized in the endosomal compartments. (H) Histogram indicates the percentage of lysosomes containing the indicated number of gold particles after 30 min of EGF uptake. Electron micrographs of ~100 lysosomes were obtained per sample, and the total number of gold particles was counted for each lysosome. Lysosomes containing more than two gold particles were counted.

phosphorylates LRRK1 on Tyr residues. Thus it is likely that EGFR associates with and phosphorylates LRRK1 at Tyr-944 following EGF stimulation. Furthermore, the phosphorylation-defective LRRK1(Y944F) mutation causes hyperactivation of LRRK1 kinase activity, suggesting that EGFR-induced Tyr-944 phosphorylation inactivates LRRK1 kinase activity. This represents a negative feedback loop by which activation of EGFR is followed by inactivation of LRRK1 that is bound to the receptor on endosomes. Indeed, we find that LRRK1 is transiently activated in response to EGF stimulation and that EGF stimulates the inactivation of LRRK1 with kinetics that correlate with Tyr-944 phosphorylation.

It was reported that LRRK1 kinase activity is governed by the binding of GTP in the ROC GTPase domain (Korr *et al.*, 2006). Consistent with this, the LRRK1(S625N) mutant lacking the GTP-binding activity is defective in kinase activity, similar to a kinase-dead LRRK1 (Hanafusa *et al.*, 2011). The phosphorylation-defective LRRK1(Y944F) mutant shows higher levels of GTP binding, whereas phosphomimic Y944E and Y944D mutations abrogate GTP binding, similar to the LRRK1(S625N) mutant. These results suggest that LRRK1 Tyr-944 phosphorylation reduces its kinase activity by affecting GTP-binding activity.

Regulation of LRRK1 kinase activity plays a critical role in the intracellular trafficking of EGFR

We previously showed that depletion of LRRK1 by siRNA disrupts the transport of EGFR from early to late endosomes (Hanafusa *et al.*, 2011). In LRRK1-depleted cells, wild-type LRRK1, but not a kinase-inactive LRRK1(K1243M), is able to restore the motility of EGF-containing endosomes, indicating that LRRK1 kinase activity is required for EGFR transport. Conversely, we here find that a hyperactive LRRK1(Y944F) mutation

causes the aberrant transport of EGF-containing endosomes toward the cell center, leading to the accumulation of EGFR in endosomes in the perinuclear region. The formation of this kind of endosome is dependent on EGF stimulation and microtubule-mediated transport. Of interest, the LRRK1(Y944F)-induced endosomal compartments appear to contain marker proteins characteristic of early, late, and recycling endosomes. In addition, electron microscopic analysis revealed that the endosomes induced by LRRK1(Y944F) fail to form proper intraluminal vesicles of MVBs. These results suggest that LRRK1 hyperactivation results in the formation of mixed endosomes in the perinuclear region due to enhanced aberrant EGFR transport.

Studies show that early endosomes move toward the cell center as they mature (Rink *et al.*, 2005; Driskell *et al.*, 2007; Woodman and Futter, 2008). During this maturation process, early endosomal markers are replaced by late endosomal markers, and recycling proteins are removed (Woodman and Futter, 2008). When endosomes have maturated sufficiently, they become competent for fusion with lysosomes. In addition, the process of endosomal maturation is coordinated with the movement of endosomes along microtubules (Soldati and Schliwa, 2006; Driskell *et al.*, 2007; Woodman and Futter, 2008). This coordination appears to be disrupted by hyperactivation of LRRK1, as expression of LRRK1(Y944F) inappropriately promotes the motility of EGF-containing endosomes. These results raise the possibility that the endosomes induced by LRRK1(Y944F) fail to mature from early to late and form proper intraluminal vesicles, and thus ultimately fail to fuse with lysosomes. Therefore the regulation of LRRK1 kinase activity might be important to ensure the orderly and timely trafficking of endosomes containing EGFR. In addition, we previously showed that LRRK1 is also required for EGFR sorting into the intraluminal vesicles of MVBs (Hanafusa *et al.*, 2011). These observations suggest that LRRK1 functions to coordinate endosomal sorting and transport, specifically for EGFR-containing endosomes during maturation. Thus our findings provide the first evidence that EGFR trafficking is regulated by a cargo-specific factor and provide a new mechanistic insight into EGFR intracellular trafficking.

MATERIALS AND METHODS

Plasmids and mutations

LRRK1(K1243M), siRNA-resistant wild-type LRRK1, and siRNA-resistant LRRK1(K1243M) were generated as described previously (Hanafusa *et al.*, 2011). LRRK1(Y944F), LRRK1(Y944E), LRRK1(Y944D), LRRK1(Y944F; K1243M), LRRK1(Y944F; S625N), and siRNA-resistant LRRK1(Y944F) were generated using the QuikChange Site-Directed Mutagenesis Kit according to the manufacturer's protocol (Stratagene, La Jolla, CA). For FLAG-tagged LRRK1, LRRK1 cDNAs were subcloned into pCMV-FLAG. Deletion constructs of LRRK1 were generated by PCR-based mutagenesis and subcloned into pEGFP-C1 (Clontech, Mountain View, CA) or pCMV vectors. The retrovirus vectors for wild-type GFP-LRRK1 and GFP-LRRK1(Y944F) were generated by insertion of LRRK1 cDNAs into the pRetroQ-AcGFP-N1 vector (Clontech).

Antibodies and reagents

Rabbit antibodies against LRRK1 were previously described (Hanafusa *et al.*, 2011). Rabbit antibodies against pTyr-944 LRRK1 were produced by MBL Medical and Biological Laboratories (Nagoya, Japan) by injecting rabbits with synthetic phosphopolypeptides, QTEEQpYFQFL (where p stands for the phosphorylated residue), coupled to keyhole limpet hemocyanin and affinity purified. Antibodies and their suppliers were as follows: anti-FLAG (M2; Sigma-Aldrich, St. Louis, MO); anti-GFP (JL-8 or full-length polyclonal antibody; Clontech); anti–phospho-Tyr (4G10; Upstate, Millipore, Billerica, MA); anti-EGFR (LA22, Upstate; or 6F1, MBL); anti-EEA1 (clone 14; BD Transduction Laboratories, Lexington, KY; and C45B10, Cell Signaling, Beverly, MA); anti–CI-MPR (2G11; Affinity BioReagents, Golden, CO); anti-LBPA (6C4; Echelon Bioscience, Salt Lake City, UT); anti-LAMP1 (H4A3, BD Transduction Laboratories); anti-GM130 (Clone 35, BD Transduction Laboratories); anti-p230 *trans*-Golgi (clone 15; BD Transduction Laboratories); and goat anti–mouse immunoglobulin G (IgG) conjugated to 10-nm gold and goat anti–rabbit IgG conjugated to 5-nm gold (BBInternational, Cardiff, United Kingdom). Rh-EGF and Alexa 647-EGF were purchased from Molecular Probes Invitrogen (Carlsbad, CA) and mouse recombinant EGF from Toyobo (Osaka, Japan).

Cell cultures, transfections, and virus infections

HeLa S3 and Cos7 cells were cultured in DMEM containing 10% fetal bovine serum. These cells were split into 35-, 60-, or 100-mm dishes at 2×10^5, 5×10^5, or 2×10^6 cells per dish, respectively. Cells were transfected using RNAiMAX (Invitrogen) or FuGENE 6 reagent (Roche Applied Science, Indianapolis, IN) according to the manufacturer's protocol. Retroviruses for expression of wild-type GFP-LRRK1 and GFP-LRRK1 (Y944F) were generated and infected into HeLa S3 cells using RetroPack Universal Packaging System (Clontech). Selection of stable cells was achieved using puromycin (Invitrogen).

Immunoprecipitation

For immunoprecipitation, cells were lysed in RIPA buffer containing 50 mM Tris-HCl (pH 7.4), 150 mM NaCl, 0.25% deoxycholic acid, 1% NP-40, 1 mM EDTA, 2 mM dithiothreitol (DTT), 1 mM phenylmethylsulfonyl fluoride, phosphatase inhibitor cocktail 2 (Sigma-Aldrich), and protease inhibitor cocktail (Sigma-Aldrich), followed by centrifugation at 15,000 × *g* for 15 min. The supernatant was added to 10 µl (bed volume) of protein G–Sepharose beads (GE Healthcare, Piscataway, NJ) or Dynabeads protein G (Invitrogen) with the indicated antibodies and rotated for 2 h at 4°C or for 10 min at room temperature. The beads were washed three times with ice-cold phosphate-buffered saline (PBS) and subjected to immunoblotting or kinase assays.

Immunoblotting

After cell extracts were subjected to SDS–PAGE (SDS–PAGE), proteins were transferred to polyvinylidene difluoride membrane (Hybond-P, GE Healthcare). The membranes were immunoblotted with various antibodies, and bound antibodies were visualized with horseradish peroxidase (HRP)–conjugated antibodies against rabbit or mouse IgG using the HRP chemiluminescent substrate reagent kit (Novex ECL; Invitrogen).

In vitro kinase assay

Immunocomplex kinase reactions of GFP-LRRK1 were performed in a final volume of 30 µl containing 50 mM 4-(2-hydroxyethyl)-1-piperazineethanesulfonic acid (pH 7.4), 5 mM $MgCl_2$, 5 mM $MnCl_2$, 0.5 mM DTT, and 5 µCi of [γ-^{32}P]ATP. Samples were incubated for 20 min at 30°C. Reactions were terminated by the addition of Laemmli sample buffer and boiling. LRRK1 was resolved by SDS–PAGE, and autophosphorylation of LRRK1 was detected by autoradiography. For kinase assay using recombinant EGFR, reactions were carried out with 0.5 mM cold ATP and 0.03 µg of recombinant EGFR (Millipore) for 5 min at 30°C. Tyrosine phosphorylation of LRRK1 was detected by immunoblotting with anti–phospho-Tyr antibodies.

GTP-binding studies

Cells were lysed in RIPA buffer containing 50 mM Tris-HCl (pH 7.4), 150 mM NaCl, 0.25% deoxycholic acid, 1% NP-40, 1 mM EDTA, 2 mM dithiothreitol, 1 mM phenylmethylsulfonyl fluoride, phosphatase inhibitor cocktail 2 (Sigma-Aldrich), and protease inhibitor cocktail (Sigma-Aldrich), followed by centrifugation at 15,000 × *g* for 15 min. Supernatants were incubated with 40 µl of a GTP-agarose bead suspension (Sigma-Aldrich) with rotation at 4°C for 2 h and then sequentially pelleted and washed three times with 1 ml of PBS. For guanine nucleotide competition experiments, GTP (Sigma-Aldrich) was added to a final concentration of 4 mM, and the incubation was continued for a further 60 min at 4°C, followed by washing. Precipitated proteins were resolved by SDS–PAGE and immunoblotted with anti-GFP antibodies.

Fluorescence microscopy

For immunofluorescence microscopy, cells grown on coverslips were treated as indicated and then fixed in 4% formaldehyde, permeabilized in 0.5% Triton X-100, and incubated with primary and secondary antibodies. Primary antibodies were anti-EEA1 at 1:100, anti–CI-MPR at 1:400, anti-GM130 at 1:100, anti-p230 at 1:100, and anti-LAMP1 at 1:2000. For LBPA staining, fixed cells were incubated with a 1:100 dilution of LBPA antibody in 0.05% saponin. Secondary antibodies were Alexa Fluor 647 goat anti–mouse IgG and Alexa Fluor 555 goat anti–mouse IgG (Molecular Probes, Invitrogen). Confocal microscopy was performed using an Olympus FV1000 microscope (Olympus, Center Valley, PA) equipped with a four-laser system (multi-argon laser, HeNe-G laser, HeNe-R laser, and LD405/440 laser diode). The excitation and emission wavelengths were 405/461 nm (4′,6-diamidino-2-phenylindole), 488/510 nm (enhanced GFP), 543/578 nm (rhodamine), 543/567 nm (Alexa 555), and 633/668 nm (Alexa 647), respectively. For each series of experiments, the microscope settings were optimized for the brightest images and were kept unaltered during the analysis. For live-cell fluorescence microscopy, cells were grown in 35-mm plastic-bottomed dishes. Time-lapse images were obtained with an Olympus FV1000 microscope. Imaging started at 15 min after the initial exposure to Alexa 647-EGF, with frames captured at 1.165-s intervals for 35 s (30 frames). Neither GFP-LRRK1 nor Alexa 647-EGF showed significant photobleaching over the 35 s of analysis. Tracking of GFP-LRRK1– and Alexa 647-EGF–positive endosomes was conducted using the Manual Tracking ImageJ plug-in (National Institutes of Health, Bethesda, MD).

RNA interference

Negative-control siRNA and stealth siRNA for human LRRK1 (target sequence, 3165gcaggaacaggaaagtcaccattta TT) were purchased from Invitrogen. Annealed siRNAs were transfected using RNAiMAX (Invitrogen). Cells were transfected with control siRNA or LRRK1 siRNA using RNAiMAX, incubated overnight, and then transfected with siRNA-resistant GFP-LRRK1 using FuGENE 6 reagent (Roche Applied Science). The transfected cells were analyzed 72 h after siRNA transfection.

Conventional electron microscopy

Conventional electron microscopy was performed as described previously (Hayashi-Nishino *et al.*, 2009), with a slight modification. After serum starvation, cells were incubated with anti-EGFR antibody (mouse monoclonal antibody LA-22; 1:350 dilution) for 2 h at 37°C, followed by goat anti–mouse IgG antibodies conjugated to 10 nm gold (BBInternational) for 1 h at 37°C in order to label endogenous EGFR on the cell surface with immunogold particles. After washing to remove antibodies from the medium, cells were stimulated with EGF for the indicated times and fixed in 4% paraformaldehyde and 1% glutaraldehyde in 0.1 M sodium phosphate buffer (PB) at pH 7.4 for 20 min. The specimens were postfixed in buffer containing 1% OsO_4 and 1.5% potassium ferrocyanide, dehydrated in a series of graded ethanol solutions, and embedded in epoxy resin. Ultrathin sections were collected and stained with uranyl acetate and lead citrate and observed under an H7600 transmission electron microscope (Hitachi, Tokyo, Japan).

Immuno–electron microscopy

The preembedding gold enhancement immunogold method was performed as described previously (Iwata *et al.*, 1995), with a slight modification. In brief, cells were fixed in 4% paraformaldehyde and 1% glutaraldehyde in PB for 20 min at room temperature. The specimens were dehydrated in a series of graded ethanols at a low temperature and embedded in LR white resin at –20°C. The resin was polymerized in a TUV-200 polymerizer (Dosaka EM, Kyoto, Japan). Ultrathin sections were cut on a microtome with a diamond knife and picked up on collodion-carbon–coated nickel grids. The grids loaded with ultrathin sections were floated on a drop of PBS–bovine serum albumin (BSA)–fetal bovine serum (FBS) (PBS containing 2% BSA and 2% FBS) for 30 min. They were then transferred to droplets (20 µl) of rabbit anti-EEA1 antibody (1:20 dilution) and mouse CI-MPR antibody (1:20 dilution) and dissolved in PBS-BSA containing 0.01% Tween 20 (PBS-BSA-T) for 60 min at room temperature. After washing with PBS-BSA-T, the specimens were incubated for 15 min with goat anti–mouse IgG conjugated to 5-nm gold and goat anti–rabbit IgG conjugated to 10-nm gold dissolved in PBS-BSA-T, washed with a 0.1 M sodium cacodylate buffer solution, and then transferred to droplets of 1% glutaraldehyde in 0.1 M sodium cacodylate buffer solution, pH 7.4, for 30 min. After washing with distilled water, ultrathin sections were stained with uranyl acetate for 10 min and with lead citrate for 1 min. They were then observed under a Hitachi H-7000 electron microscope

ACKNOWLEDGMENTS

We thank G. Takaesu and T. Kajino for technical advice and pCMV plasmids. We also thank N. Hisamoto and the members of our laboratory for their help. This research was supported by grants from the Ministry of Education, Culture, Sports, Science and Technology of Japan (to K.M. and H.H.), as well as from the Novartis Foundation, the Takeda Science Foundation, and the Naito Foundation and Astellas Foundation for Research on Metabolic Disorders (to H.H.). K.I. was supported by a Japan Society for the Promotion of Science Research Fellowship.

REFERENCES

Bosgraaf L, Van Haastert PJ (2003). Roc, a Ras/GTPase domain in complex proteins. Biochim Biophys Acta 1643, 5–10.

Citri A, Yarden Y (2006). EGF-ERBB signalling: towards the systems level. Nat Rev Mol Cell Biol 7, 505–516.

De Domenico I, McVey Ward D, Kaplan J (2008). Regulation of iron acquisition and storage: consequences for iron-linked disorders. Nat Rev Mol Cell Biol 9, 72–81.

Dikic I (2003). Mechanisms controlling EGF receptor endocytosis and degradation. Biochem Soc Trans 31, 1178–1181.

Driskell OJ, Mironov A, Allan VJ, Woodman PG (2007). Dynein is required for receptor sorting and the morphogenesis of early endosomes. Nat Cell Biol 9, 113–120.

Grant BD, Donaldson JG (2009). Pathways and mechanisms of endocytic recycling. Nat Rev Mol Cell Biol 10, 597–608.

Hanafusa H, Ishikawa K, Kedashiro S, Saigo T, Iemura S, Natsume T, Komada M, Shibuya H, Nara A, Matsumoto K (2011). Leucine-rich

repeat kinase LRRK1 regulates endosomal trafficking of the EGF receptor. Nat Commun 2, 158.
Hayashi-Nishino M, Fujita N, Noda T, Yamaguchi A, Yoshimori T, Yamamoto A (2009). A subdomain of the endoplasmic reticulum forms a cradle for autophagosome formation. Nat Cell Biol 11, 1433–1437.
Henne WM, Buchkovich NJ, Emr SD (2011). The ESCRT pathway. Dev Cell 21, 77–91.
Hurley JH (2008). ESCRT complexes and the biogenesis of multivesicular bodies. Curr Opin Cell Biol 20, 4–11.
Hurley JH, Hanson PI (2010). Membrane budding and scission by the ESCRT machinery: it's all in the neck. Nat Rev Mol Cell Biol 11, 556–566.
Hynes NE, Lane HA (2005). ERBB receptors and cancer: the complexity of targeted inhibitors. Nat Rev Cancer 5, 341–354.
Iwata K, Yamamoto A, Satoh S, Ohyama Y, Tashiro Y, Setoguchi T (1995). Quantitative immunoelectron microscopic analysis of the localization and induction of 25-hydroxyvitamin D3 24-hydroxylase in rat kidney. J Histochem Cytochem 43, 255–262.
Katzmann DJ, Odorizzi G, Emr SD (2002). Receptor downregulation and multivesicular-body sorting. Nat Rev Mol Cell Biol 3, 893–905.
Korr D, Toschi L, Donner P, Pohlenz HD, Kreft B, Weiss B (2006). LRRK1 protein kinase activity is stimulated upon binding of GTP to its Roc domain. Cell Signal 18, 910–920.
Madshus IH, Stang E (2009). Internalization and intracellular sorting of the EGF receptor: a model for understanding the mechanisms of receptor trafficking. J Cell Sci 122, 3433–3439.
Maxfield FR, McGraw TE (2004). Endocytic recycling. Nat Rev Mol Cell Biol 5, 121–132.
Miaczynska M, Pelkmans L, Zerial M (2004). Not just a sink: endosomes in control of signal transduction. Curr Opin Cell Biol 16, 400–406.
Mukhopadhyay D, Riezman H (2007). Proteasome-independent functions of ubiquitin in endocytosis and signaling. Science 315, 201–205.
Polo S, Pece S, Di Fiore PP (2004). Endocytosis and cancer. Curr Opin Cell Biol 16, 156–161.
Raiborg C, Stenmark H (2009). The ESCRT machinery in endosomal sorting of ubiquitylated membrane proteins. Nature 458, 445–452.
Rink J, Ghigo E, Kalaidzidis Y, Zerial M (2005). Rab conversion as a mechanism of progression from early to late endosomes. Cell 122, 735–749.
Sharma SV, Bell DW, Settleman J, Haber DA (2007). Epidermal growth factor receptor mutations in lung cancer. Nat Rev Cancer 7, 169–181.
Soldati T, Schliwa M (2006). Powering membrane traffic in endocytosis and recycling. Nat Rev Mol Cell Biol 7, 897–908.
Sonnichsen B, De Renzis S, Nielsen E, Rietdorf J, Zerial M (2000). Distinct membrane domains on endosomes in the recycling pathway visualized by multicolor imaging of Rab4, Rab5, and Rab11. J Cell Biol 149, 901–914.
Sorkin A, Goh LK (2009). Endocytosis and intracellular trafficking of ErbBs. Exp Cell Res 315, 683–696.
Sorkin A, von Zastrow M (2009). Endocytosis and signalling: intertwining molecular networks. Nat Rev Mol Cell Biol 10, 609–622.
Ubersax JA, Ferrell JE Jr (2007). Mechanisms of specificity in protein phosphorylation. Nat Rev Mol Cell Biol 8, 530–541.
Williams RL, Urbe S (2007). The emerging shape of the ESCRT machinery. Nat Rev Mol Cell Biol 8, 355–368.
Woodman PG, Futter CE (2008). Multivesicular bodies: co-ordinated progression to maturity. Curr Opin Cell Biol 20, 408–414.